2011 50th IEEE Conference on Decision and Control and
European Control Conference (CDC-ECC)
Orlando, FL, USA, December 12-15, 2011

Cascade Mitigation in Energy Hub Networks

Mads Almassalkhi Ian Hiskens

Abstract— **The paper establishes a formulation for energy hub networks that is consistent with mixed-integer quadratic programming problems. Line outages and cascading failures can be considered within this framework. Power flows across transmission lines and pipelines are compared with flow bounds, and tripped when violations occur. The outaging of lines is achieved using a mixed-integer disjunctive model. A model predictive control (MPC) strategy is developed to mitigate cascading failures, and prevent propagation of outages from one energy-carrier network to another. The MPC strategy seeks to alleviate overloads by adjusting generation and storage schedules, subject to ramp-rate limits and governor action. If overloads cannot be eliminated by rescheduling alone, MPC determines the minimum amount of load that must be shed to restore system integrity. The MPC strategy is illustrated using a small 12 hub network and a much larger network that includes 132 energy hubs.**

I. INTRODUCTION

Recent large-scale power grid failures have placed a renewed focus on the reliability and optimality of energy supply systems [1]. Such systems extend beyond electrical power to include many different energy carriers, such as natural gas, hydro, and wind energy. In fact, coupling energy carriers may reveal vulnerabilities and minimum cost solutions that are not apparent when each energy system is treated separately [2]. We employ energy hubs and move beyond the traditional view to consider large-scale coupled energy systems. An energy hub represents a relatively new and general concept in power systems, which explicitly models couplings between multiple energy networks [3], [4].

In this paper, we are specifically interested in large-scale cascading failures,which have been studied extensively in decoupled electrical networks [5], [6], [7]. However, research on cascading failures in large coupled systems generally does not consider the concept of energy hubs [8].

Employing the optimization framework developed in [9], we construct large energy hub systems and investigate these systems under multi-line outages. Power flows across transmission lines and pipelines will be compared against proper flow bounds, and when violations occur, the lines will be taken out of service (tripped). There exists a myriad of approaches to determine when an overloaded line should be tripped, ranging from deterministic hard constraints with memory, as in [10], to soft-constrained probabilistic setups described in [11]. Incorporation of line-tripping into our model is accomplished by employing a mixed-integer disjunctive model [12]. To mitigate the effects of a disturbance and prevent cascading failures, we employ a model predictive controller to minimize load shedding.

This work was supported by U.S. Department of Energy under research grant DE-SC0002283.

M. Almassalkhi and I. Hiskens are with Department of Electrical Engineering: Systems, University of Michigan, 1301 Beal Avenue Ann Arbor, MI 48109, U.S.A. {malmassa, hiskens}@umich.edu

TABLE I
VARIABLES THAT ARISE IN THE ENERGY HUB MODEL.

Variable Type	Variables
Decision	$\mathbf{s}, \mathbf{f}_D, \widehat{\mathbf{P}}, \mathbf{f}_G$
Dependent	$\mathbf{x}, \mathbf{P}, \mathbf{L}, \mathbf{f}, , \mathbf{E}, \dot{\mathbf{E}}$
Constant Parameter	$\mathbf{C}, \eta_{ch}, \eta_{dis}$

Our paper is organized as follows. In Section II, we formulate the energy hub network and disjunctive line-outage models. In Section III, we discuss our model predictive control (MPC) scheme for cascade mitigation. The model predictive controller is employed in Section IV to mitigate the effect of a cascade failure in two different energy hub networks. Section V presents the simulation results, while section VI concludes the paper with remarks on future work.

II. MODEL

Multi-carrier energy networks can be formulated in many ways. This paper will focus the discussion on the "hybrid energy hub" model developed in [4] and [13]. Table I categorizes the variables that arise in the model and they are described in the following subsections. The decision variables are those quantities that a system controller could directly manipulate. In our model, we can control line-switching, load-shedding and converter, generator, and energy storage utilization. For more details on the models in sections II-A and II-B, we refer the reader to [9].

A. Energy Hub Model

Most common energy hubs can be constructed from interconnections of five simple building blocks: input sources, input storage, converters, output storage, and output sources. In describing the flow of power from hub input to hub output, we need to consider the flow between each of the five blocks of the hub. Let $h \in \mathscr{H}$ be a hub from the set of available hubs, where h has input sources $i \in \{1, 2, \ldots, N_{in}\}$ and output sources $n \in \{1, 2, \ldots, N_{out}\}$. Let P_i be the input flow from source i at hub h. Referring to Fig. 1(a), to describe the flow from input source i to a converter j, we have to take into account any input storage devices and possible dispatch factors. The dispatch factors $\nu_{ij} \in [0, 1]$ determine the dispatch flows $\widehat{P}_{ij}$, which describe the amount of input flow i that is directed to converter j.

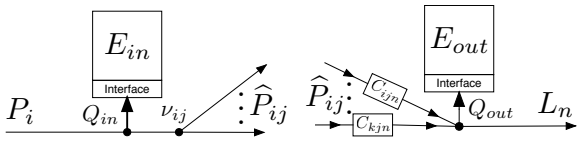

(a) From input to converters. (b) From converters to output.

Fig. 1. Decomposing the energy hub model based on dispatch flows.

From Fig. 1(a), we see that

$$P_i = Q_i^{in} + \sum_{j=1}^{k_i} \widehat{P}_{ij}, \tag{1}$$

where Q_i^{in} is the flow going into input storage device i and $\widehat{P}_{ij}$ is one of the k_i flows determined by the dispatch factors, ν_{ij}, such that

$$\widehat{P}_{ij} = \nu_{ij}(P_i - Q_i^{in}) \tag{2}$$

and

$$\sum_{j=1}^{k_i} \nu_{ij} = 1, \qquad 0 \le \nu_{ij} \le 1. \tag{3}$$

Note that (3) ensures conservation of flow between input storage and converter blocks. Employing (2) and (3), we can eliminate dispatch factors ν_{ij} to obtain

$$0 \le \widehat{P}_{ij} \le P_i - Q_i^{in}. \tag{4}$$

Referring to Fig. 1(b), output flows L_n are obtained by converting dispatch flows $\widehat{P}_{ij}$. Converter C_{ijn} converts the j-th dispatch flow of input source i into output source n. The output flows L_n must also take into account any output storage device flow, Q_n^{out}. Thus, modeling hub output flows gives,

$$\sum_i \sum_{j \in \mathcal{D}(i,n)} C_{ijn} \widehat{P}_{ij} = Q_n^{out} + L_n, \tag{5}$$

where $\mathcal{D}(i,n)$ is the set of dispatch flows from input i that can be converted to output n, and $|\mathcal{D}(i,n)| \le k_i$.

With regard to input and output energy storage devices, we must consider multiple time periods since energy source p, stored at time $t \in \{1, 2, \ldots, T\}$, depends on the power available in the previous time step. If we assume steady-state storage power values, a constant slope for $\dot{E}_p = dE_p/dt$, and treat storage interface as a converter device with charging and discharging efficiencies η_{ch} and η_{dis}, the relationship between storage flows Q and the change in energy levels is

$$\dot{E}_p = \frac{dE_p}{dt} \approx e_p Q_p, \tag{6}$$

where

$$e_p = \begin{cases} \eta_{ch}, & \text{if } Q_p \ge 0 \quad \text{(charge/standby)} \\ 1/\eta_{dis}, & \text{if } Q_p < 0 \quad \text{(discharge)} \end{cases} \tag{7}$$

which yields for the energy storage level,

$$E_p^t = E_p^{t-1} + \dot{E}_p^t. \tag{8}$$

Since a storage device has two distinct states of operation, charging and discharging, that achieve different efficiencies, energy storage devices introduce switches in the energy hub formulation. To avoid this nonlinearity, we make use of binary variables to distinguish between the two states. Let the steady-state storage power flow be defined by the sum of a positive (charging) and a negative (discharging) power flow, such that

$$Q_p = Q_{p,ch} + Q_{p,dis}, \tag{9}$$

with

$$-(1 - x_p)\underline{Q}_p \le Q_{p,dis} \le 0 \tag{10}$$

$$0 \le Q_{p,ch} \le x_p \overline{Q}_p, \tag{11}$$

where $x_p \in \{0, 1\}$, and $\overline{Q}_p$ and $\underline{Q}_p$ are limits on the flow into and out of device p. Thus, when $x_p = 0$, storage device p is in discharging mode (as $Q_{p,ch} \equiv 0$), while $x_p = 1$ implies p is in charging mode (with $Q_{p,dis} \equiv 0$). We can now write $\dot{E}_p$ in terms of $Q_{p,ch}$ and $Q_{p,dis}$ as,

$$\dot{E}_p = \eta_{ch} Q_{p,ch} + \frac{1}{\eta_{dis}} Q_{p,dis}. \tag{12}$$

Notice that (6) is nonlinear because it involves the product of two state variables, e_p and Q_p. Equation (12) is an equivalent linear description. Therefore, by introducing additional binary variables x_p, we have removed a nonlinearity. We can now rewrite (8) in terms of the charging and discharging variables, giving

$$E_p^t = E_p^{t-1} + \eta_{ch} Q_{p,ch}^t + \frac{1}{\eta_{dis}} Q_{p,dis}^t. \tag{13}$$

Note that because we explicitly take dispatch flows into account and employ binary variables to descripe energy storage, we employ a strictly linear formulation of hub h. Furthermore, since no two hubs share components or dispatch flows, each hub is decoupled and the description of $\mathscr{H}$ is straightforward.

B. Interconnection of Energy Hubs

Energy hubs are interconnected via various energy supply networks. In the previous section, we defined how power flowed through an energy hub from input to output. To describe the flow of power between hubs, we need to include power networks. A power network is a simple graph with additional physical constraints corresponding to the specific nature of the network, e.g. electrical or natural gas. Let $\mathscr{G} = (\mathscr{N}, \mathscr{A})$ be a simple graph with nodes $\mathscr{N} = \{1, 2, \ldots, N\}$ and arcs $\mathscr{A} = \{1, 2, \ldots, E\}$. Define the sets of generator and load nodes as $\mathscr{C}$, $\mathscr{D} \subset \mathscr{N}$, respectively, where generator nodes inject power into the network while load nodes consume power from the network. The remaining nodes are called throughput nodes and neither inject nor consume power. Every graph must satisfy flow balance. That is, the sum of flows into and out of node i must equal the flow injected f_{G_i}, or consumed $-f_{D_i}$, at node i. Thus, for each node i of each network we have,

$$\sum_{j \in \mathcal{C}(i)} f_{ij} = b_i = \begin{cases} f_{G_i} & i \in \mathscr{C} \\ -f_{D_i} & i \in \mathscr{D} \\ 0 & \text{otherwise} \end{cases} \tag{14}$$

where $\mathcal{C}(i)$ is the set of nodes connected to node i, and f_{ij} is positive (negative) for flow out of (into) node i.

With the inclusion of energy hubs, we need to consider flows between energy hubs and networks, and (14) becomes,

$$\sum_{j\in\mathcal{C}(i)} f_{ij} = b_i - \sum_{l\in\mathcal{H}(i)} P_l + \sum_{m\in\mathcal{H}(i)} L_m, \tag{15}$$

where $\mathcal{H}(i)$ is the set of hubs connected to node i, P_l is the power input to hub l, and L_m is the power output from hub m. Note that the coupling between energy hubs and power networks only takes place at hub inputs and outputs.

Besides being connected to energy hubs, the main difference between a graph and a power network lies in additional constraints arising from the physical nature that underlies the energy type of a network. For example, the added constraints imposed on an electrical power network often come in the form of the linear DC flow model,

$$f_{ij}x_{ij} - (\theta_i - \theta_j) = 0, \tag{16}$$

where x_{ij} is the reactance of arc (i,j) and θ_i is the phase angle at node i [14]. The physical constraints are generally nonlinear, however. A common nonlinear physical constraint is seen with natural gas networks, where the power flow through pipelines depends in a nonlinear manner on the pressure, p_i, applied at the nodes,

$$f_{ij} = \begin{cases} k_{ij}\sqrt{p_i - p_j}, & \text{if } p_i \geq p_j \\ -k_{ij}\sqrt{p_j - p_i}, & \text{if } p_i < p_j \end{cases} \tag{17}$$

where k_{ij} is a constant pertaining to the specific gas and pipeline properties [15].

We will denote the physical constraints of any network n by an equation of the form:

$$\mathbf{\Gamma}_n(\mathbf{f}, \xi_n, \mathbf{A}_n) = 0, \tag{18}$$

where ξ_n are the state variables associated with the physical constraints, and $\mathbf{A}_n$ is the node-arc incidence matrix for network n. Note that $\mathbf{\Gamma}_n$ is independent of the energy hubs.

In this paper, for simplicity, we assume no frictional resistance between pipelines and gas, so compressors are not considered and we linearize all nonlinear constraints about nominal values.

C. Line-outages

If the power flow, f_{ij}, exceeds the recommended flow limit, u_{ij}, it can permanently damage arc (i,j). Therefore, sensors are often placed on arcs in a power grid to automatically take lines out of service when they exceed their flow limits. For example, in electric grids, transmission lines have a flow limit that is based on the thermal limit of the conductor to prevent excessive and dangerous sagging and permanent damage. In this paper, it is assumed that lines can withstand an overload for T_F minutes before sustaining permanent damage and being taken out of service. The process of taking lines out of service is often called "line-tripping."

To allow the controller of the system to trip lines, we need to modify the formulation of arc flows to establish an equivalent mixed-integer disjunctive formulation. When an arc is removed, no power can flow across the arc, which naturally lends itself to the utilization of binary integers on flow bounds:

$$-(1 - s_{ij})u_{ij} \leq f_{ij} \leq (1 - s_{ij})u_{ij}, \tag{19}$$

where $s_{ij} \in \{0,1\}$ for all $(i,j) \in \mathscr{A}$ and $s_{ij} = 1$ if arc (i,j) is taken out of service (tripped). However, due to the physical constraints (16), we need to perform additional modifications so those constraints are inactive when corresponding arcs are tripped. Applying the disjunctive formulation to the linear DC flow constraint (16) gives:

$$|f_{ij}x_{ij} - (\theta_i - \theta_j)| \leq Ms_{ij}, \tag{20}$$

where M is a large number. Thus, for $s_{ij} = 0$, we get the constraint in (16), but when the line is tripped and $s_{ij} = 1$, we have $f_{ij} = 0$ from (19). It follows that (20) reduces to:

$$|\theta_i - \theta_j| \leq M. \tag{21}$$

If M is sufficiently large, we have effectively made constraint (16) inactive for arc (i,j), as the phase angle difference between nodes i and j is approximately unbounded, which is to be expected if there was no arc connecting the two nodes. Using (18), we can easily extend the disjunctive formulation to any general network n, and the following formulation is employed when we consider line-tripping:

$$|\mathbf{f}| \leq \mathbf{u} \cdot (\mathbf{1} - \mathbf{s}), \tag{22}$$

$$|\mathbf{\Gamma}_n(\mathbf{f}, \xi_n, \mathbf{A}_n)| \leq M\mathbf{s}, \tag{23}$$

for all networks n. Any additional constraints arising from specific networks have similar disjunctive formulations. One advantage of incorporating the line-outage model into the existing formulation is that we can set up and solve for the power flow, even when the system is split into multiple islands.

It should be cautioned, however, that optimizing with respect to binary vector $\mathbf{s}$ for large M-values can greatly slow down integer programming solvers and lead to numerical round-off errors [5].

D. Economic Dispatch in Energy Hubs

Under normal operating conditions, we consider the energy hub system on the slow timescale, t, which consists of one-hour time-steps. The system is operated according to an economic dispatch schedule computed off-line from the Multi-Period Optimal Dispatch Formulation described in detail in [9]. In short, we satisfy forecasted nominal demand and minimize the cost of generation by optimal utilization of available hub storage and expected externally injected power (for example wind power) from hour 1 to hour T: $MinGenCost(1{:}T)$ in Fig. 2. The schedule acts as our reference signal and informs the operator how to employ generators ($\mathbf{f}_G$), hub dispatch flows ($\hat{\mathbf{P}}$), and hub storage devices ($\mathbf{Q}_{in}$ and $\mathbf{Q}_{out}$), whether lines should be taken out of service ($\mathbf{s}$), and how much demand to satisfy ($\mathbf{f}_D$). These quantities represent our *decision variables*. The main differences between the (Schedule) and (Real-time)

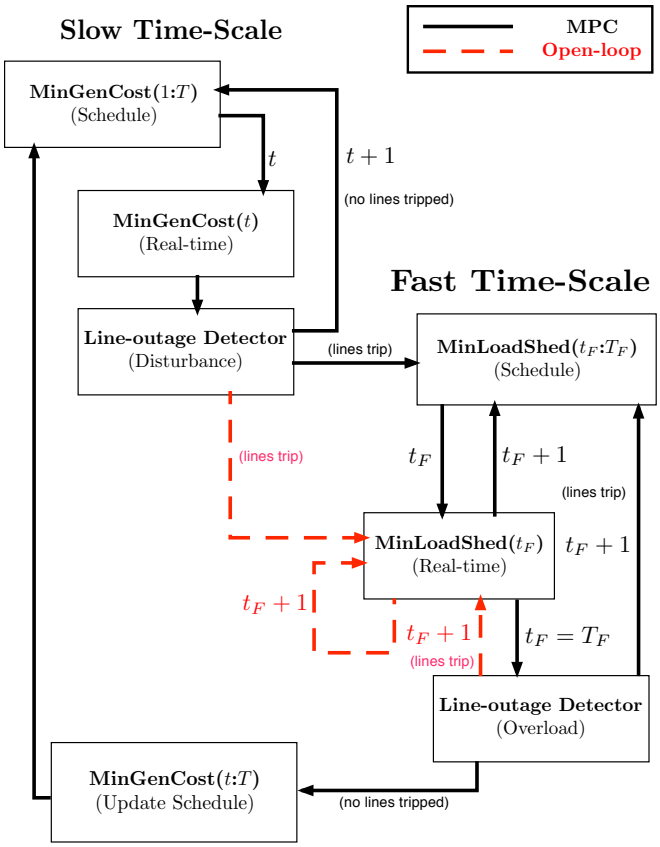

Fig. 2. Flow diagram of the implementation of cascade mitigation model

MinGenCost blocks in Fig. 2 arise from the constraint sets. In the (Schedule) block, we calculate the minimum generation cost subject to arc flow limits over T periods; however, for the (Real-time) block, we fix the decision variables according to the schedule's recommendations at time t (single period), and compute the resulting power flows with flow limit constraints inactive. If the (Schedule) has a perfect model of the (Real-time) system, arc flows will always be within their limits.

III. CASCADE MITIGATION

Cascade failures occur when an initial disturbance to the system (i.e. unexpected line-outages) forces a redistribution of flows that overloads additional lines, which leads more lines to go out-of-service. If left uncontrolled, the cycle of line-outages and redistribution of flows is referred to as a cascade failure.

There are two general approaches to mitigating cascade failures in power networks. The first method attempts to predict the disturbance *a priori* and is based on off-line computation of all possible failures in the network and control policies to deal with each possible failure. A major drawback of this approach is that it does not scale well with the size of the network. Modified versions of this approach attempt to compute only a small subset of the most likely or most damaging failures, but since the space of possible failures in a network is very large, such methods fall victim to the colloquial saying about "finding a needle in a haystack." The second method is based on retroactive control, whereby the uncertainty surrounding the disturbance has been revealed and one can utilize the knowledge available about the disturbance to develop control algorithms in real-time to mitigate the effects of the disturbance. This paper focuses on the latter approach and considers a model predictive control (MPC) scheme that operates as shown in Fig. 2.

Once a disturbance occurs and lines are taken out of service, operation is switched to the fast timescale, t_F, which consists of one-minute time-steps. During the fast timescale nominal load and intermittent power injections are fixed at their most recent slow timescale values.

The MPC algorithm *MinLoadShed*$(t_F{:}T_F)$ undertakes a multi-period optimization to determine a schedule for generation and storage that achieves minimal load shedding. The optimization takes into account ramp rates [14] and governor action [16], to ensure the proposed schedule is consistent with the behavior of the real system. In Fig. 2, the real system is modeled by *MinLoadShed*(t_F).

Following a disturbance, MPC establishes the optimal response over the subsequent period of T_F minutes. The formulation assumes that lines can withstand an overload for T_F minutes, but if the overload persists beyond that time then the line will trip. MPC seeks to remove all overloads by adjusting generation and storage over the horizon up to T_F. If overloads remain at that time, however, then the final MPC action is to shed minimum load.

When MPC is first initiated by a detected disturbance (i.e. line trip), it considers the entire horizon of T_F minutes, determines the optimal generation and storage schedules, and communicates the first instance of that schedule to the real system, *MinLoadShed*(t_F). One minute later, MPC receives measurements from the system, possibly from a state-estimator, which become the starting point for determining a new schedule over the remaining $(T_F - 1)$ minute horizon. The first instance of that new schedule is again communicated to the real system, and the process repeats. The horizon shrinks by one minute each iteration until time T_F is reached. If all line overloads have not been cleared at that time, MPC determines the minimum load shedding required to avert line tripping, and communicates those values to the loads. If the MPC model perfectly matches the real system, no overloads will remain, and the cascade will be halted. On the other hand, if the MPC model is not perfect, some overloads may remain. If so, those lines will trip, signaling MPC to repeat the entire process. This continues until no further line tripping occurs. At that point, the slow-timescale economic dispatch schedule is updated with the latest values for generation, storage, and load via *MinGenCost*$(t{:}T)$, and the optimal schedule over the remainder of the 24 hour period is determined. Without the look-ahead feature of MPC, a closed-loop controller acting at time T_F would shed more load as it would not be able to properly allocate storage utilization to overcome possible future generator ramping limits.

For the open-loop case, shown in red in Fig. 2, the arc

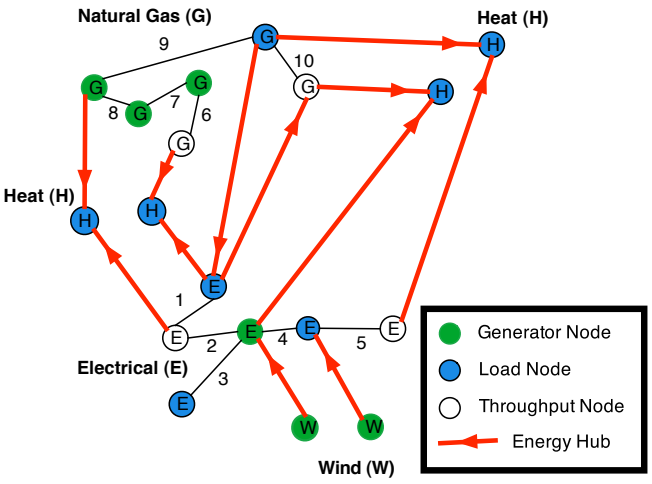

Fig. 3. Network representation of small 12-hub system

flows are given by the power flow solution with no regard for flow limits. Thus, the open-loop problem may undergo significant cascading failures.

IV. SIMULATION

The formulation of energy hubs described in [9] permits the construction of arbitrarily large interconnected energy hub networks and, together with CPLEX and MATLAB, allows implementation of our model predictive cascade mitigation approach discussed in Section III and outlined in Fig. 2.

In this paper, we investigate the effects of a disturbance on small and large energy hub systems. Because current power grid operating and planning standards ensure power systems are in a reliable condition even if one contingency occurs [1], our disturbance will consist of multiple simultaneous outages. Each system consists of an electrical network, a natural gas network, district heat loads, wind turbines, and multiple energy hubs that couple the four different energy types. The smaller system is useful in describing how our model predictive approach mitigates a cascade failure, while the large system allows us to better showcase the effects of cascade mitigation.

To construct both energy hub networks, we employ the technique proposed in [17] for building random grids. The technique assumes uniform node location, exponential expected link length distribution, and Poisson distribution for arc selection. The parameters used to construct the power grids are in per unit (p.u.) and provided in Table II. The small energy hub system is shown in Fig. 3. Due to the size of electrical and natural gas networks and the random interconnectivity with energy hubs, a meaningful visualization of the large energy hub system is not straightforward and is excluded. However, via application of graph drawing software, such as Tulip [18], visualization is a possibility for the future.

The topological characteristics of our systems are given in Tables III and IV. The values N, E, G, and D represent the number of nodes, arcs, generators, and loads, respectively, while $\langle k \rangle$ is the average nodal degree. The wind and heat networks have no arcs and consist exclusively of generators and loads, respectively. We employed 12 energy hubs in the small system and 132 energy hubs in the large system to couple the four power networks. The energy hubs are used to connect from the electrical network to gas (via electrolysis) and heat networks (via resistor heating), from the gas network to electrical (via gas turbines and fuel cells) and heat networks (via furnaces), and from the wind network to the electrical network (via turbines). All other network couplings, for example from gas to wind and from heat to electric, are excluded in this simulation. Table V shows the energy conversion efficiencies employed in our simulation. Note that the efficiency between wind energy and electric energy is set to 1.0, because we only consider injected power from the wind generators and the lossy conversion between wind speed and generator is assumed to have already taken place. All hubs connecting the wind network to the electrical

TABLE II
PARAMETERS FOR CONSTRUCTION OF RANDOM GRIDS

Parameters	Value/Bounds	Units
Electric Generators	[20,25]	p.u.
Gas Generators	[20,25]	p.u.
Wind Generators	[0, 6]	p.u.
Electric Loads	[0.5, 2]	p.u.
Gas Loads	[0.5, 2]	p.u.
Heating Loads	[1,2]	p.u.
Arc Flow Limits	[2, 4]	p.u.
Generator Ramping Limits	40	p.u./hr
Storage Ramping Limits	40	p.u./hr

TABLE III
TOPOLOGICAL CHARACTERISTICS OF THE 12-HUB ENERGY NETWORK

Network	$\langle k \rangle$	N	E	G	D
Electrical	1.67	6	5	1	3
Gas	1.67	6	5	3	1
Wind	0	2	0	2	0
Heat	0	4	0	0	4

TABLE IV
TOPOLOGICAL CHARACTERISTICS OF THE 132-HUB ENERGY NETWORK

Network	$\langle k \rangle$	N	E	G	D
Electrical	4.36	100	218	28	37
Gas	4.30	100	214	20	41
Wind	0	30	0	30	0
Heat	0	40	0	0	40

TABLE V
CONVERSION EFFICIENCIES BETWEEN ENERGY TYPES

From \ To	Electric	Gas	Wind	Heat
Electric	–	0.80	–	0.75
Gas	0.70	–	–	0.90
Wind	1.0	–	–	–
Heat	–	–	–	–

network have limited output storage, while hub (input or output) storage is added randomly to 75% of the remaining hubs.

The system is assigned 24 one-hour time-intervals ($T = 24$), corresponding to one complete day of operation. For the fast timescale, network arcs are allowed to be overloaded for no more than 5 minutes before being tripped automatically ($T_F = 5$). The consumer demand (load) is set to peak near midday, while wind power is available mostly in the early and later parts of the day. The cost of generation (electric and natural gas) is set to vary along with forecasted demand, so generation near midday is more expensive than during the earlier or later parts of the day. Electric generation is set to be more expensive than natural gas.

The disturbance takes place at a random time between hours 1 and 24, unknown to the system controller, and consists of simultaneous outage of multiple lines. For the small energy hub system, the disturbance takes out 3 lines, while the larger network experiences a simultaneous outage of 5 lines.

V. SIMULATION RESULTS

The small and large systems described in section IV were simulated according to the flow diagram in Fig. 2.

A. Small 12-hub system

For the small system shown in Fig. 3, the disturbance takes place at time $t = 7$ when three lines are taken out of service. Prior to the disturbance, the optimal dispatch schedule is computed off-line and is implemented as expected. Due to the cost of generation peaking during midday, cheap generation is employed to maximize storage utilization early in the day, as shown in Fig. 4 (b and c). Then after 7 hours, the disturbance causes the simultaneous outage of lines 2, 5, and 8. Within 5 minutes, our MPC approach reconfigures generation and energy storage (taking account of ramping limits) to satisfy nominal demand. However, in the fifth minute, as we seek to enforce the flow limits, we are forced to shed around 20% of total load - mainly from the electrical load supplied by line 1 ($\sim 70\%$ shed), but the gas load supplied by line 9 ($\sim 25\%$) and the upper rightmost heating loads ($\sim 30\%$ each) are affected as well. Line 9 is crucial to the system, as it allows us to mitigate the effects of the disturbance through hub connections.

Since the MPC halts further line outages, control returns to the slow timescale and a new schedule is computed to minimize generator costs over the remainder of the 24-hour period. When wind power peaks towards the end of the day, despite having three lines out of service, we are able to restore loads as shown in Fig. 4(a) and, therefore, reject the disturbance. Energy hubs play an important role in this problem, because the storage devices and hub-couplings of networks provide flexibility in the optimal scheduling of power flows to limit line overloads.

For the open-loop case, without the fast timescale MPC, we cannot reconfigure generation to enforce flow limits after the disturbance. Thus, in the fifth minute, the important line 9 is overloaded (as no load has been shed) and it trips from service. With the loss of line 9, we cannot supply the electric load supplied by line 1 and the gas load supplied by line 9 (both 100% shed). The upper rightmost heating loads utilize stored energy at maximal rates to avoid having to be shed. At hour 8, around 40% of load is shed in the system and at hour 9, when no stored energy remains to supply the upper-right heating loads, they are shed completely, resulting in $\sim 50\%$ of total load being shed. As seen in Fig. 4(a), the load is not restored in the remaining time.

Since we were interested in control policies that shed minimal load, load-shedding was heavily penalized in our formulation. Therefore, when load-shedding occurred during the "MPC" and "open-loop" problems, the costs shown in Fig. 4(d) became less a measure of minimal generation costs and more a measure of how much load was shed during each problem.

B. Large 132-hub system

For the larger system, described in Table IV, the disturbance also takes place at time $t = 7$, when five lines are removed from service. Prior to the disturbance, the schedule computed off-line is employed to schedule generation and storage. As was the case with the small system, the low cost of generation during the early parts of the day leads to maximal storage utilization. After 7 hours, the disturbance causes the simultaneous outage of 5 randomly chosen lines. Within 5 minutes, our MPC approach reconfigures generation and energy storage (taking into account ramping limits) to satisfy nominal demand across the new network. In the fifth minute, arc flows are returned to within their limits without having to shed any load. This is because a larger system with more nodes, arcs, and generators has greater flexibility in routing power flows to satisfy nominal demand.

With a larger network, however, the complexity increases and it becomes more difficult to understand where weaknesses lie and how the system will respond to a disturbance. For the open-loop problem, a cascading failure occurs as a consequence of the initial loss of five lines. For the next 115 minutes, the system utilizes all available hub storage to desperately avoid shedding load, as shown in Fig. 5(c). But as lines are tripped due to overloads, more and more load is shed. Fig. 5(a-b) provides a fast timescale view of the cascading effect of outages and load shedding. The cascade comes to an end when load-shedding has significantly lowered generation output levels, such that arc flows are within limits. In fact, the total load shed immediately after the cascade, when wind is low, is around 40%, Later in the day, when wind power has increased, some of the load is restored ($\sim 30\%$ shed).

The generator levels in Fig. 5(d) show that our model predictive controller rejects the disturbance by returning to optimal pre-disturbance levels at time $t = 17$. At $t = 24$, the small difference between generation levels of the "MPC" and "No Disturbance" problems is due to excess available wind energy, which allows flexibility in the optimal solution. That is, in the final time-step, either excess (free) wind energy

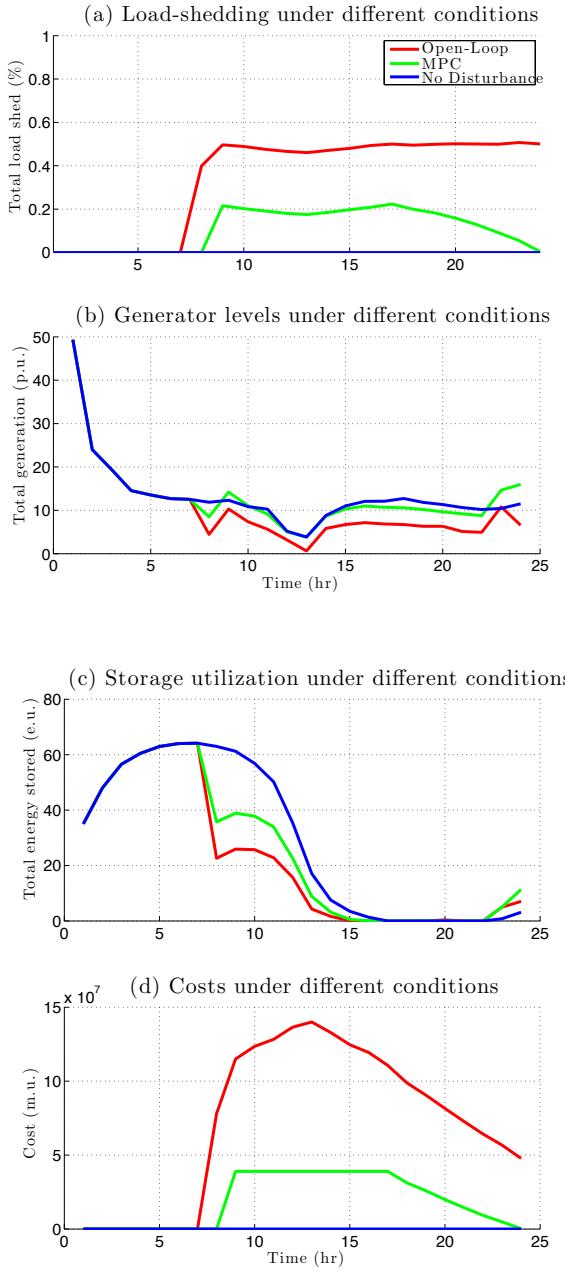

Fig. 4. Simulation results from small 12-hub system

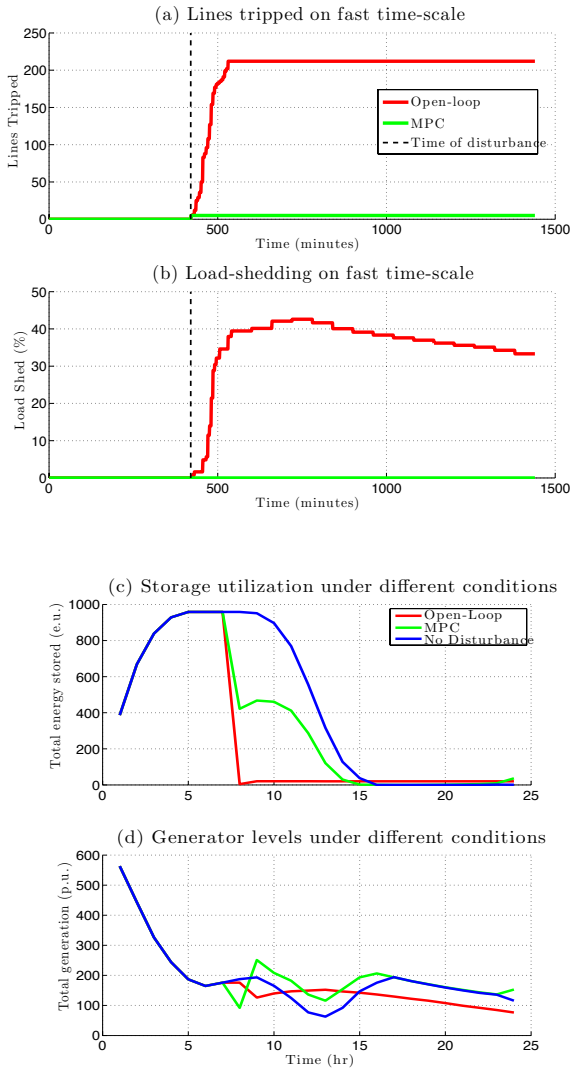

Fig. 5. Simulation results from large 132-hub system

can be stored or wind generation curbed. Both solutions are optimal because stored energy has no future value. Thus, the MPC approach presented in this paper minimizes load shed and mitigates the effects of disturbances in general energy hub systems.

VI. CONCLUSIONS AND FUTURE WORK

In this paper, we have developed an MPC approach to mitigate the effects of cascades in arbitrarily large energy hub networks. We accomplished this by incorporating line outages into the economic dispatch formulation and operate the system on a fast timescale to minimize load-shedding after a disturbance.

Further studies will improve upon the line outage model to include probabilistic outage rates determined by cumulative line overloads. Taking into account the entire horizon in the multi-period formulation can lead to very large optimization problems. Therefore, future work will focus on applying decomposition techniques to allow larger networks to be solved more efficiently. Finally, with energy hub networks in mind, we will pursue theoretical developments to analyze the robustness and stability of large complex networks and investigate distributed model predictive control strategies.

REFERENCES

[1] U.S.-Canada Power System Outage Task Force, "Final report on the August 14, 2003 blackout in the United States and Canada: causes and recommendations," 2004.

[2] M. Geidl, G. Koeppel, P. Favre-Perrod, B. Klockl, G. Andersson, and K. Frohlich, "Energy hubs for the future," *Power and Energy Magazine, IEEE*, vol. 5, no. 1, pp. 24 – 30, 2007.

[3] H. Groscurth, T. Bruckner, and R. Kümmel, "Modeling of energy-services supply systems," *Energy*, vol. 20, no. 9, pp. 941–958, 1995.
[4] M. Geidl and G. Andersson, "A modeling and optimization approach for multiple energy carrier power flow," *In Proc. of IEEE PES PowerTech, St. Petersburg, Russian Federation*, pp. 1 – 7, 2005.
[5] D. Bienstock and A. Verma, "The n-k problem in power grids: New models, formulations, and numerical experiments," *SIAM Journal on Optimization*, vol. 20, p. 2352, 2010.
[6] H. Ren and I. Dobson, "Using transmission line outage data to estimate cascading failure propagation in an electric power system," *Circuits and Systems II: Express Briefs, IEEE Transactions on*, vol. 55, no. 9, pp. 927 – 931, 2008.
[7] A. Pinar, J. Meza, V. Donde, and B. Lesieutre, "Optimization strategies for the vulnerability analysis of the electric power grid," *SIAM Journal on Optimization*, vol. 20, no. 4, pp. 1786–1810, 2010.
[8] S. Buldyrev, R. Parshani, G. Paul, H. Stanley, and S. Havlin, "Catastrophic cascade of failures in interdependent networks," *Nature*, vol. 464, no. 7291, pp. 1025–1028, 2010.
[9] M. Almassalkhi and I. Hiskens, "Optimization framework for the analysis of large-scale networks of energy hubs," *Power Systems Computation Conference*, 2011.
[10] D. Bienstock and S. Mattia, "Using mixed-integer programming to solve power grid blackout problems," *Discrete Optimization*, vol. 4, pp. 115–141, 2007.
[11] B. Carreras, V. Lynch, M. Sachtjen, I. Dobson, and D. Newman, "Modeling blackout dynamics in power transmission networks with simple structure," *36th Hawaii International Conference on System Sciences*, 2001.
[12] L. Bahiense, G. Oliveira, and M. Pereira, "A mixed integer disjunctive model for transmission network expansion," *IEEE Transactions on Power Systems*, vol. 16, no. 3, pp. 560–565, 2001.
[13] A. del Real, M. Galus, C. Bordons, and G. Andersson, "Optimal power dispatch of energy networks including external power exchange," *European Control Conference 2009 in Budapest, Hungary*, vol. 9, 2009.
[14] A. Wood and B. Wollenberg, *Power Generation, Operation, and Control*. Wiley-Interscience, second ed., 1996.
[15] A. Osiadacz, *Simulation and Analysis of Gas Networks*. Gulf, first ed., 1987.
[16] A. Bergen and V. Vittal, *Power Systems Analysis*. Prentice Hall, second ed., 2000.
[17] Z. Wang, R. Thomas, and A. Scaglione, "Generating random topology power grids," *Proceedings of the 41st Hawaii International Conference on System Sciences*, pp. 1–9, 2008.
[18] D. Auber and F. Jourdan, "Interactive refinement of multi-scale network clusterings," *Proceedings of Ninth International Conference on Information Visualisation*, pp. 703 – 709, 2005.